Australasian Physical & Engineering Sciences in Medicine (2019) 42:757–769
https://doi.org/10.1007/s13246-019-00775-0

SCIENTIFIC PAPER

A new fast algorithm to achieve the dose uniformity around high dose rate brachytherapy stepping source using Tikhonov regularization

H. Badry[1] · L. Oufni[1] · H. Ouabi[2] · H. Iwase[3] · L. Afraites[4]

Received: 5 April 2019 / Accepted: 2 July 2019 / Published online: 30 July 2019
© Australasian College of Physical Scientists and Engineers in Medicine 2019

Abstract

The dose optimization algorithm based on anatomical points is developed to produce rapidly uniform doses over target distances generated on the target volume edges in high-dose-rate (HDR) brachytherapy stepping source application for a treatment length of 6 cm. Monte Carlo modeling of the ^{60}Co HDR brachytherapy source and the surrounding medium were performed using PHITS code. The source dwell times were optimized using Tikhonov regularization in order to obtain uniform dose distribution at the anatomical points located at predefined target distances. The computed dose rates at distances from 0.25 up to 20 cm away from the source were first verified with the literature data sets. Then, the simulation results of the optimization process were compared to the calculations of commercial treatment planning system (TPS) SagiPlan. As a result, the dose uniformity was observed in the isodose curves at the target distances of 10 and 15 mm of the treatment length and the prescribed dose achieved the anatomical points uniformly. The algorithm developed in the present study can be applied for achieving the dose uniformity around the brachytherapy stepping source as a quicker tool for different treatment lengths and different target distances while maintaining the high quality of the treatment plans, saving time by avoiding the manual isodose shaping and then better suitable treatment for patients.

Keywords High-dose-rate · Stepping-source · Dose-optimization · Tikhonov

Introduction

Cancer can be treated with different irradiation methods, externally or internally [1]. In the external therapy, the tumor is irradiated from different directions outside from the patient's body, like intensity modulated radiation therapy using a linear accelerator [2]. In internal radiation therapy, called brachytherapy, the patients are treated with the sealed radioactive source placed very close or in contact with the target tissue. The high dose rate (HDR) brachytherapy is performed with remote afterloading systems, where the source is welded to the end of a transfer cable, which is small enough to move freely through a catheter. The various types of available brachytherapy sources vary according to their geometry and the isotope selected (^{192}Ir, ^{125}I, ^{60}Co, ^{252}Cf…) [3–5]. The development of small single source projectors, able to define a programmed series of dwell times and positions and offered the possibility to adjust the time by position. The optimization of these parameters offers the possibility to modify the dose distribution in order to find an optimal treatment plan (dose plan), which satisfy the clinical goals.

A single catheter with linear geometry implant is often used in the treatment of cancerous lesions in cervix, esophagus, rectum and endobronchial cancer [6]. The stepping source within the catheter in brachytherapy applications is used to treat a tumor lesion that is longer than the effective treatment length of the source [7, 8]. One of the main challenges in brachytherapy is to select the optimal combination for particular treatment parameters to produce dose distribution that best conforms to the purpose of the

✉ L. Oufni
oufni@usms.ma; loufni@gmail.com

1 Department of Physics (LPM-ERM), Faculty of Sciences and Techniques, Sultan Moulay Slimane University, B.P. 523, 23000 Béni-Mellal, Morocco

2 Oncology Center Al Azhar, Rabat, Morocco

3 Applied Research Laboratory, KEK, High Energy Accelerator Research Organization, 1-1 Oho, Tsukuba, Ibaraki 305-0801, Japan

4 Laboratory of Mathematics and Applications, Faculty of Sciences and Techniques, Sultan Moulay Slimane University, B.P. 523, 23000 Béni-Mellal, Morocco

clinical treatment. The optimal sequence of dwell times and positions of the stepping source are determined using the information of the patient's anatomy and the position of the implanted catheter. Moreover, to achieve the desired dose distribution, anatomical points can be generated relative to the target volume that cover the specific area to be irradiated, and then the desired dose is prescribed at these points.

In order to find the treatment plan which best matches the clinical goals, the inverse planning or forward planning can be used. In forward planning, the dose plan is obtained manually using various tools available in the treatment planning system software. The resulting dose distribution is evaluated according to clinical goals for the volumes of interest and repeatedly adjusted until comes close enough to the clinical purpose. Inverse planning instead starts with the desired criteria and then a plan is computed that satisfies these criteria as well as possible. For inverse planning, mathematical optimization is commonly used [9].

The mathematical models for dose optimization must, therefore, lead to a correct coverage of the target volume, to homogeneity as high as possible in the target volume and a rapid decrease in the dose outside this volume. Several mathematical models for dose optimization have been proposed for dose planning in brachytherapy, can be found in, for example, Morén et al. [9], Lahanas et al. [10], Giantsoudi et al. [11], and Holm et al. [12] and an overview in De Boeck et al. [13]. This paper considers such models which have not been established before in brachytherapy applications, the mathematical model is referred to Tikhonov regularization. This method has been applied for the inverse treatment planning in the radiotherapy optimization problems by many research groups [14–16].

The purpose of this study was to investigate the dose rate distribution around HDR brachytherapy source. Moreover, this study presents a mathematical algorithm where the clinical objectives are defined as mathematical equations for developing the treatment plan of a high dose rate brachytherapy application. The regularized solution of the inverse problem using Tikhonov regularization allows for a quick generation of the treatment plans in order to obtain correct coverage of the target volume with the smoothest dose distribution while sparing normal tissues.

Materials and methods

Geometry of the stepping source

The BEBIG ^{60}Co source model Co0.A86 is made of an active Cobalt cylinder with a density of 8.9 g/cm^3. Its active length and diameter are 3.5 and 0.5 mm, respectively. The active core of the source is incorporated in a thin air gap of 1 mm and converted by 316L stainless steel capsule with 8.04 g/cm^3 density. The percentage of the elemental composition by weight of the capsule is C (0.03%), N (0.75%), Si (0.045%), P (0.045%), S (0.03%), Cr (17%), Mn (2%), Fe (65.543%), Ni (12%) and Mo (2.5%). The details of the source geometry can be found in Badry et al. [17].

TPS dose calculations

In this study, SagiNova afterloader machine equipped with a source of Cobalt-60 was used. The software used for the HDR remote afterloading system is SagiPlan TPS (version 1.0), it was designed and developed by Eckert & Ziegler BEBIG in Germany. This software version allows the manual and automatic optimization with a variety of tools and manual isodoses shaping. It can reconstruct one or more applicators and calculate the optimal dose distribution based on the contoured volumes and prescribed dosage. SagiPlan TPS of the SagiNova machine is currently being used for BEBIG ^{60}Co HDR brachytherapy practice at Al Azhar Oncology Center in Rabat, Morocco.

The dosimetric parameters of the source; the radial dose function, $g_L(r)$, and the anisotropy function, $F(r, \theta)$, were extracted from this treatment planning system.

Monte Carlo calculation

To calculate the dose distribution around the stepping source, we employed the Particle and Heavy Ion Transport code System (PHITS) version 3.02 running on the Ubuntu operating system at the Applied Research Laboratory of the High Energy Accelerator Research Organization, KEK. In PHITS package, a graphical utility (ANGEL) is included for the visualization of the obtained results as well as the setup geometries used for simulations [18]. PHITS has proven its applicability in various fields related to space radiation dosimetry, heavy ion radiotherapy and medical physics [19–21].

To confirm whether the PHITS computation results were reliable, we performed a computation for the radial dose function, and then the obtained results were compared with the literature data [22] and with the extracted values from TPS. Dose calculations are based on the American Association of Physicists in Medicine Task Group No. 43U1 (AAPM-TG43U1) formalism [23]. The source was placed in the center of the water phantom while the longitudinal axis was along the Z-axis. In addition, cylindrical rings concentric to the longitudinal axis of the source with similar height and thickness of 0.05 cm, for the distance ranging from 0.25 to 20 cm were used as scoring zones. On the other hand, a grid system composed of small spheres of different radii were located at selected radial distances and angles in order to obtain the anisotropy function. The simulated angle θ increases from the source tip to the cable side of the source

from 0° to 179°. The simulations were performed for 5×10^8 photons histories and the maximum of Monte Carlo statistical errors was 0.8%.

To obtain the dose distribution around the stepping source, a cubic geometry mesh with a dimension of $2\times2\times2$ mm^3 was used; this cubic mesh corresponded to a plane in the longitudinal direction of the source with the dimension of 20×20 cm^2. The simulations were carried out using the (*RI*) source function in PHITS code, where the source was considered isotopic with an activity of 62 GBq. The tally *T-Deposit* was used to score the energy being deposited in the mesh by electron produced from photon interaction. The results of this tally were normalized in unit of second by setting the parameter *norm* to zero in the section of the source definition. The simulations were performed with the Electron Gamma Shower computation mode by setting the parameter *negs* to one. The cutoff energies of 10 keV and 100 keV were applied for photons and electrons, respectively. A total number of 5×10^8 photon histories were scored for each source step of the treatment length.

Dose calculation around the stepping source

Dose distribution around the stepping source was calculated to obtain the isodose curves in the longitudinal plan for the treatment length of 6 cm. The source stops at 25, 13 and 7 dwell positions in 2.5, 5 and 10 mm steps, respectively. The anatomical points were generated at 10 and 15 mm directly away from the center of the source for each dwell position. The prescribed dose that should receive all the anatomical points was chosen to be 6 Gy.

Figure 1 shows the geometry of the stepping source and the anatomical point P, located at a distance d from the source center at each position. The received dose by these points is the sum of the product of the dwell time and the corresponding dose rate of the source at every dwell position.

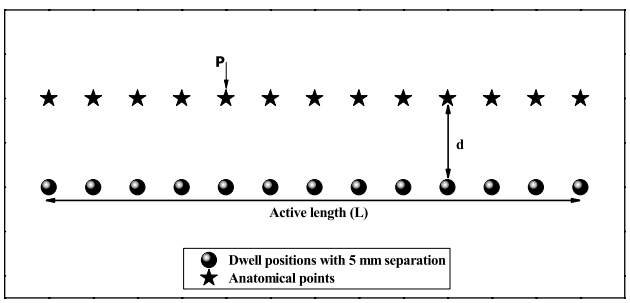

Fig. 1 Example for location of the anatomical point (P) relative to 13 dwell positions with 5 mm separation for the treatment length of 6 cm. d is the distance between P and the center of the source center at each dwell position

Optimization algorithm

For a given number of n_t dose points, each of these points receives a dose contribution of m_t dwell positions, the optimization problem can be expressed by the minimization of χ^2 between the prescribed and calculated doses:

$$\chi^2 = \sum_{i}^{n_t} \left(D_{i,p} - D_{i,c}\right)^2 \tag{1}$$

where $D_{i,p}$ is the dose prescribed in point i. $D_{i,c}$ is the dose calculated at point i.

The calculated dose at point i from each position j of the source is:

$$D_{i,c} = \sum_{j=1}^{m_t} D_{i,j} \times T_j \tag{2}$$

where $D_{i,j}$ is the dose rate in (Gy/s) at the anatomical point i at the dwell position j for the corresponding dwell time T_j in (s).

The dose matrices were obtained for each dwell position separately in PHITS calculation since the length of the source is greater than the distance between two successive dwell positions for 2.5 mm step.

Let D be the dose matrix of size $n_t \times n_t$ obtained by PHITS calculations and T is the dwell times vector of size n_t. The linear system Eq. (2) can be describe as shown in the Eq. (3):

$$D \cdot T = D_c \tag{3}$$

where D_c is the calculated dose vector of size n_t.

The linear system expressed in Eq. (3) can be described as the product of dose matrix and vector of dwell time values. This kind of linear problem is referred to the inverse problems, i.e., problems that require the determination of the unknown input to a linear system from the known output. In our case, the unknown inputs are the dwell times and the known output is the prescribed dose at the anatomical points (6 Gy). The solution of our inverse problem is therefore to find the dwell times of the source at each position in order to deliver uniform dose (100% of the reference dose of 6 Gy) along the treatment length.

The dose matrix D is ill-conditioned since its calculated condition number was about 10^3. The computation of useful approximation of T can be accomplished by replacing the linear system of Eq. (3) by a nearby system. This replacement is referred to Tikhonov regularization by introducing a stabilization parameter, this method has been widely used [24–26].

The Tikhonov regularization method replaces the ill-posed problem in Eq. (3) by a minimization problem whose the general form is:

$$\min_T \left\{ \|DT - D_c\|_2^2 + \lambda \|L(T - T_0)\|_2^2 \right\} \quad (4)$$

where λ is a positive constant called the regularization parameter that determines the amount of regularization and to control the solution vector, L represents the first or second derivative operator, which is chosen to incorporate desirable properties on the solution, T_0 is an estimated solution for a priori information. Here and below χ^2 denotes the 2-norm.

In general, choosing T_0 as zero and L as an identity matrix gives a standard Tikhonov regularization form:

$$\min_T \left\{ \|DT - D_c\|_2^2 + \lambda \|T\|_2^2 \right\} \quad (5)$$

For any fixed λ, the system in Eq. (5) has a unique solution can be expressed as:

$$T_\lambda = (D^{\mathrm{T}} D + \lambda I)^{-1} D^{\mathrm{T}} D_c \quad (6)$$

where D^{T} is the transpose of the dose matrix D.

In order to solve Eq. (5), the dose matrix D can be decomposed by means of Singular Value Decomposition (SVD) as follows to give a further survey to the solution.

$$D = U \sum V^{\mathrm{T}} = \sum_{i=1}^{n_t} u_i \sigma_i v_i^{\mathrm{T}} \quad (7)$$

where Σ is a diagonal matrix with the singular values, satisfying: $\sum = diag(\sigma_1 \ldots \sigma_n), \sigma_1 \geq \sigma_2 \geq \ldots \geq \sigma_n \geq 0$ and the matrices U and V consist of left and right singular vectors $U = (u_1 \ldots u_2), V = (v_1 \ldots v_2)$.

Tikhonov solution of Eq. (6) can now be given using SVD as:

$$T_\lambda = \sum_{i=1}^{n_t} f_i \frac{u_i^{\mathrm{T}} D_c}{\sigma_i} v_i \quad (8)$$

where $f_i = \frac{\sigma_i^2}{\sigma_i^2 + \lambda}, i = 1 \ldots n_t$ being the Tikhonov filter factors.

The determination of a suitable value of the regularization parameter λ is an important task. In the literature, there exist several procedures to estimate an optimal regularization parameter value for the inverse problem. These methods aimed to choose the regularization parameter that can controls the degree of regularization applied to the problem and then satisfies some criteria or obtains a parameter that minimize functions [27–29]. In this study, the L-curve method was used for choosing the regularization parameter λ [30–32].

For this purpose, the residual norm $\|DT_\lambda - D_c\|_2$ and solution norm $\|T_\lambda\|_2$ were calculated and plotted in a log–log scale diagram for several regularization parameters. The norm of regularization solution and corresponding residual can be calculated as:

$$\|T_\lambda\|_2^2 = \sum_{i=1}^{n_t} \left(f_i \frac{u_i^{\mathrm{T}} D_c}{\sigma_i} v_i \right)^2 \quad (9)$$

$$\|DT_\lambda - D_c\|_2^2 = \sum_{i=1}^{n_t} \left((1 - f_i) \sigma_i^{\mathrm{T}} D_c \right)^2 \quad (10)$$

The optimal value of the regularization parameter λ can be found in the vicinity of the L-curve corner constructed by the regularized norm and the residual norm, presented in log–log plot, where both values achieve their minimum that satisfy the clinical purpose of the present study which is the minimization between the prescribed and the calculated doses.

In order to assess the treatment plans developed in the present study, the cumulative dose–volume histograms (DVHs) were obtained from the SagiPlan brachytherapy TPS based on the optimized dwell times resulting from the Tikhonov regularization method.

Results

The radial dose function of the BEBIG ^{60}Co HDR source was estimated using the output files of PHITS code. The dose distribution was calculated along the transverse axis of the source and normalized by the dose obtained at the reference point, as described in the TG-43 formalism [23], which is located 1 cm from the source center. The radial dose function values were tabulated (Table 1) and presented in Fig. 2 for distances ranging from 0.25 to 20 cm.

To validate the results of the PHITS calculations, a comparison was made with published data [22] and the extracted values from SagiPlan TPS. Moreover, to illustrate this comparison the ratio $\frac{g_L(\mathrm{r})_{[\mathrm{reference}]}}{g_L(\mathrm{r})_{[\mathrm{this\ work}]}}$ was used and the results are presented in the Fig. 3.

The calculated anisotropy function at selected radial distances ranging from 0.5 to 8 cm and angles from 0° to 179° are presented in Fig. 4.

The dose distributions related to the treatment length of 6 cm in the longitudinal plane of the BEBIG ^{60}Co HDR stepping source were obtained by PHITS code for each step. Our calculations were performed to achieve uniform dose distribution at the anatomical points for the target distances of 10 mm and 15 mm. The Eq. (8) was solved for several values of λ with the dose matrix obtained for each step in PHITS calculation. Then, the calculated solution norm $\|T_\lambda\|_2$ versus residual norm $\|DT - D_c\|_2$ were presented in a log–log scale diagram (Fig. 5). The corner

Table 1 Monte Carlo calculated values of the radial dose function

r (cm)	$g_L(r)$		
	This work	Badry et al. [22]	SagiPlan TPS
0.25	1.057	1.069	1.007
0.5	1.031	1.027	1.036
0.75	1.007	1.015	1.015
1	1.000	1.000	1.000
1.5	0.991	0.993	0.992
2	0.986	0.987	0.984
3	0.970	0.967	0.968
4	0.953	0.950	0.952
5	0.933	0.931	0.936
6	0.918	0.920	0.919
7	0.901	0.902	0.902
8	0.884	0.882	0.884
9	0.869	0.865	–
10	0.848	0.844	0.849
12	0.815	0.811	0.813
15	0.756	0.754	0.756
20	0.665	0.664	0.665

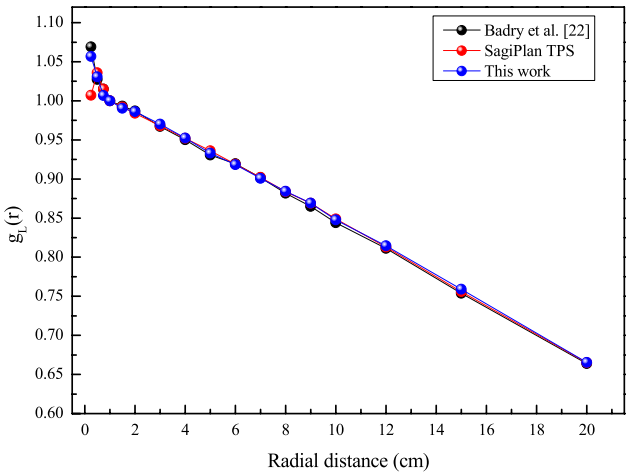

Fig. 2 Radial dose function calculated by PHITS code in water

coordinates of the L-curve plot were marked by a red circle, which correspond to the optimal regularization parameter of 0.0065 and 0.0050 for the target distances of 10 and 15 mm, respectively. Table 2 summarizes the regularization parameters obtained for the treatment length with various source steps and target distances. As a result, the regularized solutions obtained using Tikhonov regularization which correspond to the optimal dwell times for the treatment length of 6 cm, with the stepping size of 2.5, 5 and 10 mm, were plotted in Fig. 6. Finally, the optimal dwell times were multiplied by the dose matrices of each dwell position and the isodose curves were obtained using ANGEL (Fig. 7). In these figures, the isodose curves of 10, 25, 50, 100, 200 and 500% were plotted.

The Cumulative DVHs were obtained from the SagiPlan brachytherapy TPS based on the optimization process and presented in the Fig. 8. The reference volumes of 20.43 and 43.85 cm^3 for the target distances of 10 and 15 mm, respectively, are the volume encompassed by the reference isodose (100%).

Discussion

In high dose rate brachytherapy, the source dwell positions and times are vital parameters in achieving desirable dose distribution. Inverse planning requires an optimal choice of these parameters to achieve the correct coverage of the target volume with the lowest receivable dose to normal cells.

In this study, the radial dose function and dose uniformity of the source was evaluated by the application of dose optimization technique around the HDR stepping source of ^{60}Co along the target distances for a treatment length of 6 cm with various source steps. Achieving the dose uniformity of the source at predefined anatomical points can increase the efficiency of treatment.

For the radial dose function, the statistical errors of Monte Carlo calculations increase as the radial distance increases and the number of histories remains constant. The results of the reference data correlate well with the obtained values in the present work, the only exception was observed at the radial distance of 0.25 cm, where the calculated relative differences were about 4.93% and 1.14% comparing to the extracted data from SagiPlan TPS and to results reported by Badry et al. [22], respectively.

The results of the anisotropy function show good agreement with the extracted values from SagiPlan TPS. The values decrease as θ approaches the longitudinal axis of the source. This can be explained by the increase of source tip encapsulation and the source cable on the other side.

The calculated values of the anisotropy function on both sides of the reference polar angle of 90° are mirror images of each other since the source is considered symmetrical relative to the transverse plane as described in TG-43 formalism. However, the values for $\theta > 150$ were lower than those of $\theta < 30$, this asymmetry can be explained by the effect of the source cable length.

The largest differences occur at distances close to the source, and these differences decrease as the distance increases from the source center. It can be explained by the variation of the dose distribution nearby the source, due to the higher photon attenuation at this zone.

The L-curve method was applied to evaluate the inverse problem of brachytherapy dwell times. The results presented in Fig. 5 show that the optimal value of the regularization

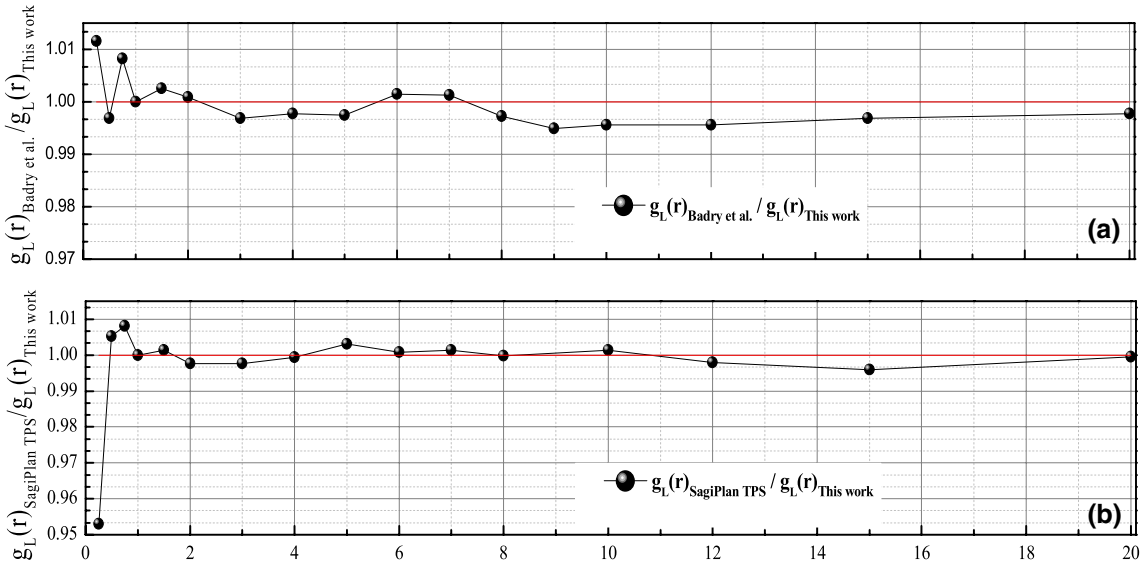

Fig. 3 The ratio $g_L(r)_{[Reference]} \Big/ g_L(r)_{[This\ work]}$ for the comparison of radial dose function. **a** Comparison with Badry et al. [22]. **b** Comparison with SagiPlan TPS

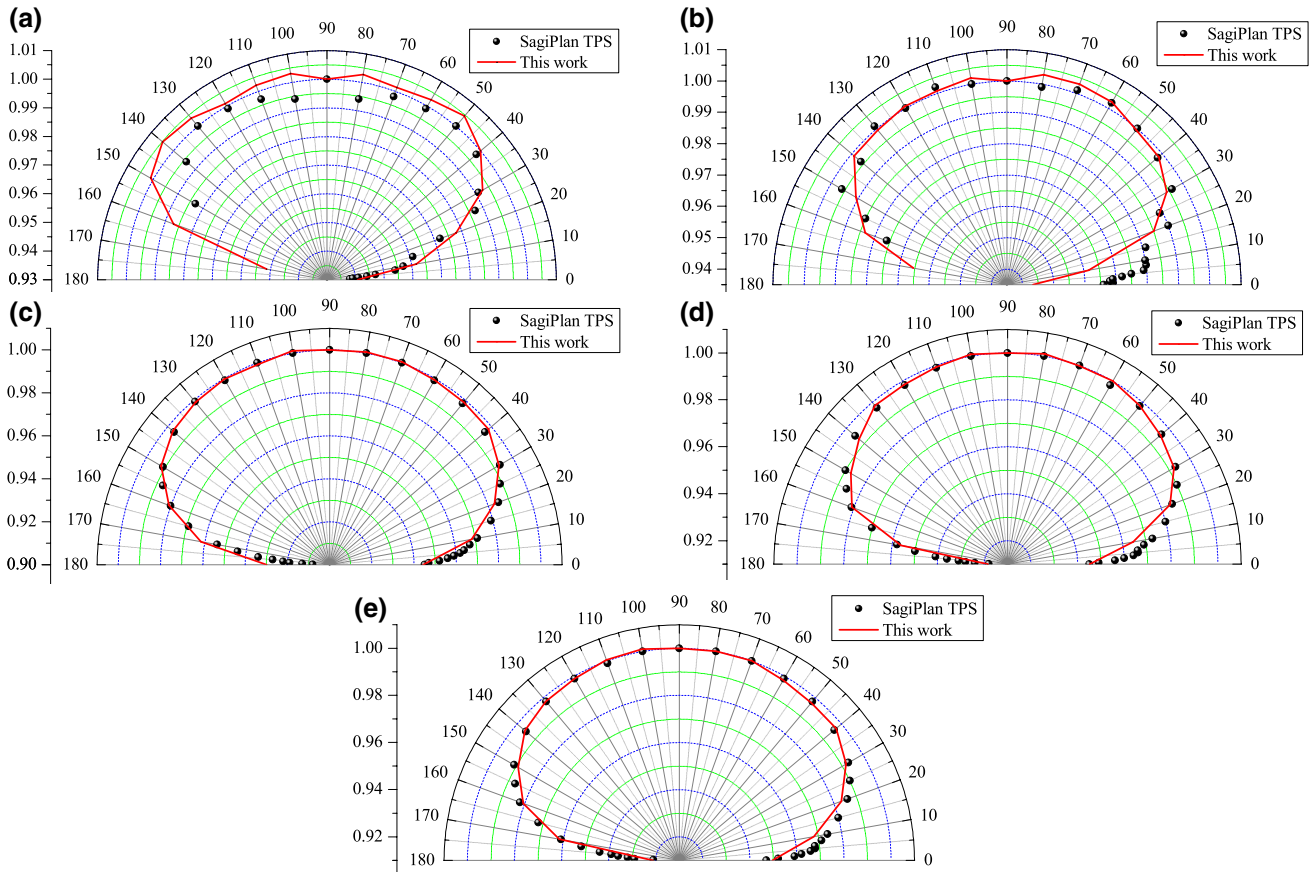

Fig. 4 The anisotropy function for selected radial distances. a = 0.5 cm, b = 0.75 cm, c = 1.5 cm, d = 6 cm, e = 8 cm

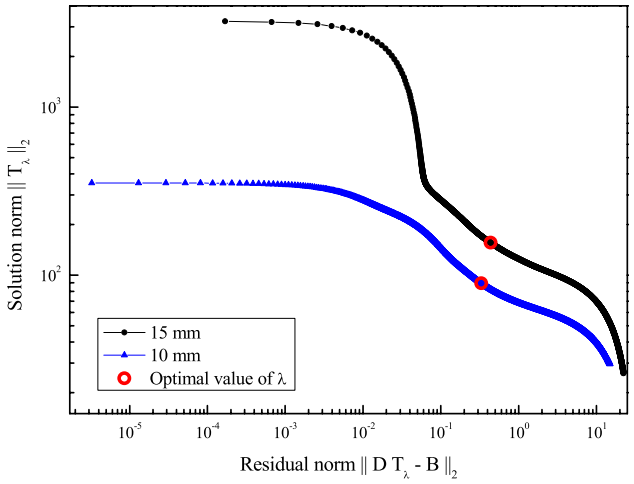

Fig. 5 L-curve plots in log–log scale for the treatment length of 6 cm with 2.5 mm source step for the target distances of 10 and 15 mm. The corner corresponding to the point of the optimal regularization parameter is marked by the red circle, it occurs for 0.0065 and 0.0050 for the target distances of 10 and 15 mm, respectively

Table 2 Regularization parameters for the treatment lengths of 6 cm with various source steps and target distances

Target distance (mm)	Treatment length of 6 cm		
	Stepping size (mm)		
	2.5	5	10
10	0.0065	0.003	0.0002
15	0.0050	0.0029	0.0001

parameter was located nearby and not at the corner of the L-curve plot. This can be explained by the effect of the physical regularization; the dwell time constraints (i.e. all the regularized solutions must be greater than 0.3 s). The obtained solutions calculated from the Eq. (8) were different from the ones obtained in Eq. (3) using the simple matrix computation, which include negative solutions. However, a small amount of control by regularization parameter values makes a marked difference.

The results of Fig. 6 display that the dwell time profiles reach their maximum at the first and the last dwell position. Therefore, it takes a longer time to deliver the required dose at both ends than at the middle dwell positions. The doses at the middle positions are almost compensated by the dwell positions nearby.

As can be seen in Fig. 7, the results demonstrate that the L-curve method can provide effective solutions to the inverse problem of our studied cases, which is revealed in the isodose curves of the treatment length of 6 cm with the various source steps, furthermore, the isodose curve of 100% cover all the anatomical points. Therefore, the correct coverage of the target volume with the smoothest dose distribution and a uniform dose around the BEBIG ^{60}Co HDR stepping source were achieved.

To verify the practical use of the developed algorithm in this study, the optimal dwell times resulting from the optimization process were used as input parameters for SagiPlan TPS and the isodose curves were generated for the same percentages of doses as obtained above. The calculated doses at the anatomical points were obtained and compared to the Monte Carlo calculations (Table 3). For the target distances of 10 mm, the average dose differences between TPS and MC calculations were about 1.01, 1 and 1.5% for the stepping size of 2.5, 5 and 10 mm, respectively. Moreover, for the target distances of 15 mm, the average dose differences were about 1.06, 1.18 and 1.04% for the stepping size of 2.5, 5 and 10 mm, respectively.

As shown in DVHs plots (Fig. 8), any point on the curve shows the volume that receives the indicated dose. For the source step of 2.5 mm and the target distance of 15 m, the whole target volume received at least 99.85% of the prescription dose, whereas 97.7% of the target volume will receive the prescription dose (6 Gy). Table 4 summarizes the DHV parameters obtained for the treatment length with various source steps and target distances, including, $V_{100\%}$ (volume receiving 100% of the prescribed dose) and $D_{100\%}$ (dose received by 100% of the target volume).

Conclusion

In the present study, the BEBIG ^{60}Co HDR brachytherapy stepping source model Co0.A86 was simulated using PHITS code. The radial dose function and the anisotropy

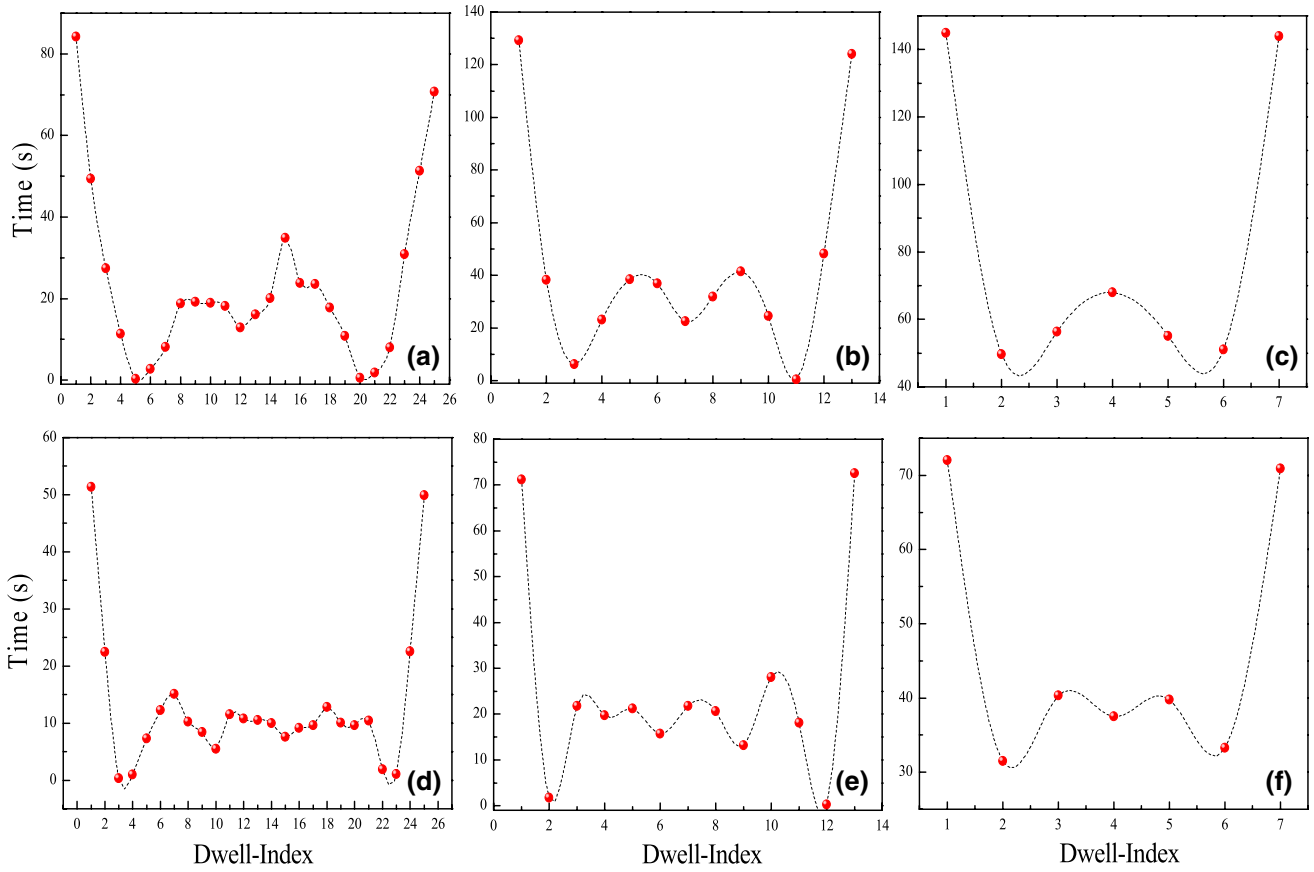

Fig. 6 Dwell time profiles for the treatment length of 6 cm. **a–c** For target distance of 15 mm. **d–f** For the target distance of 10 mm with 2.5, 5 and 10 mm step, respectively

function were calculated and compared to the extracted value from SagiPlan TPS and to the literature data.

A method based on Tikhonov regularization was used to solve the inverse problem which yields optimal dwell times for delivering uniform dose to the anatomical points located at the target distances. The results of the mathematical model were used as input parameters in TPS and the calculated doses at the anatomical points were compared to Monte Carlo calculations. Therefore, the results were in good agreement within 1.5%. Moreover, the prescription dose achieves the anatomical points uniformly along the treatment length.

The clinicians could avoid the manual shaping of isodoses to prepare the treatment plans using the algorithm developed in the present study, while maintaining the high quality of the treatment plans, saving time and then better suitable treatment for patients. In addition, the present algorithm can be extended for different treatment lengths and target distances.

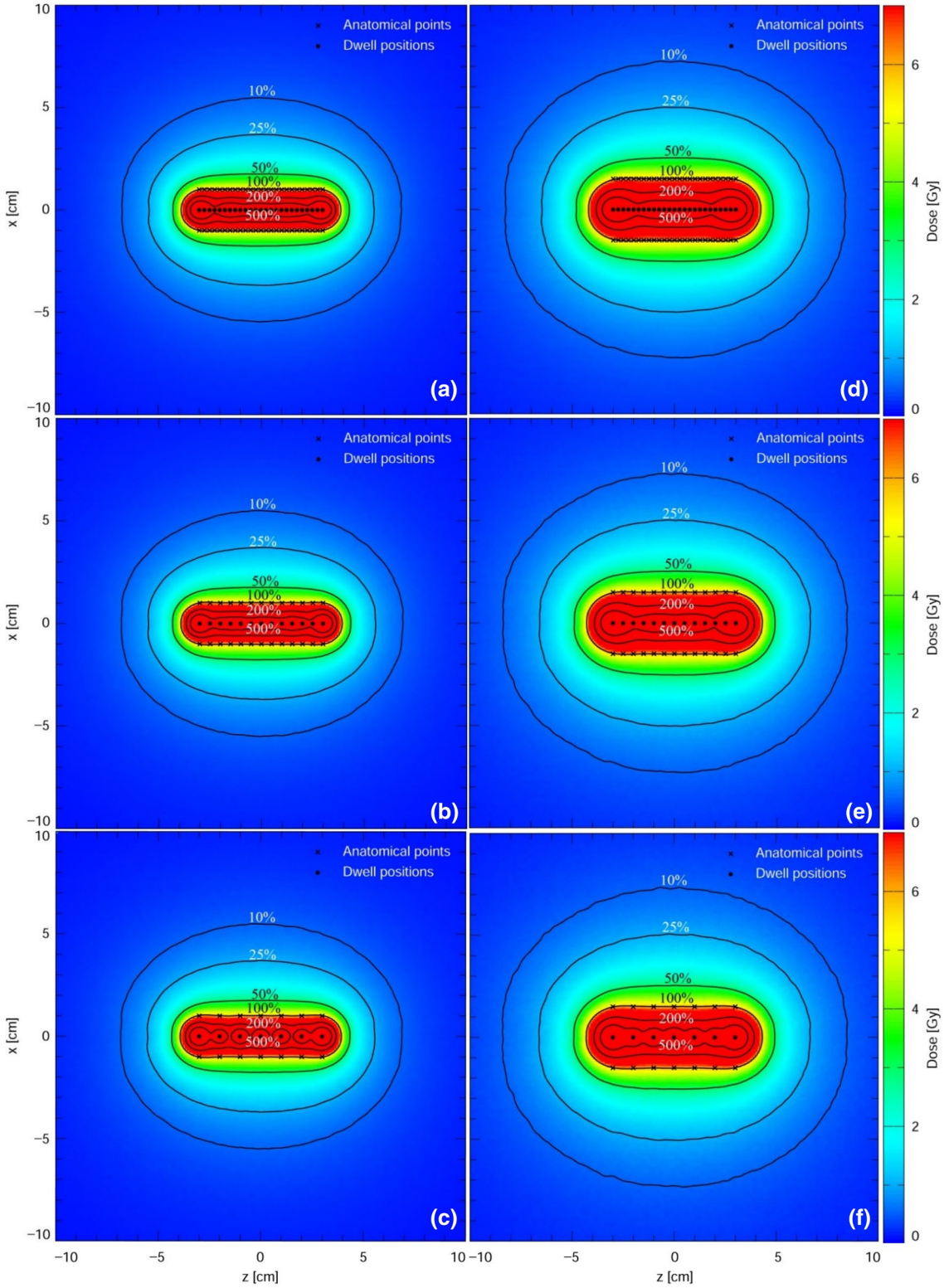

Fig. 7 Isodose curves (10, 25, 50, 100, 200 and 500%) around the BEBIG ^{60}Co HDR stepping source for the treatment length of 6 cm with source steps of 2.5, 5 and 10 mm. **a–c** For target distance of 10 mm. **d–f** For the target distance of 15 mm with 2.5, 5 and 10 mm step, respectively

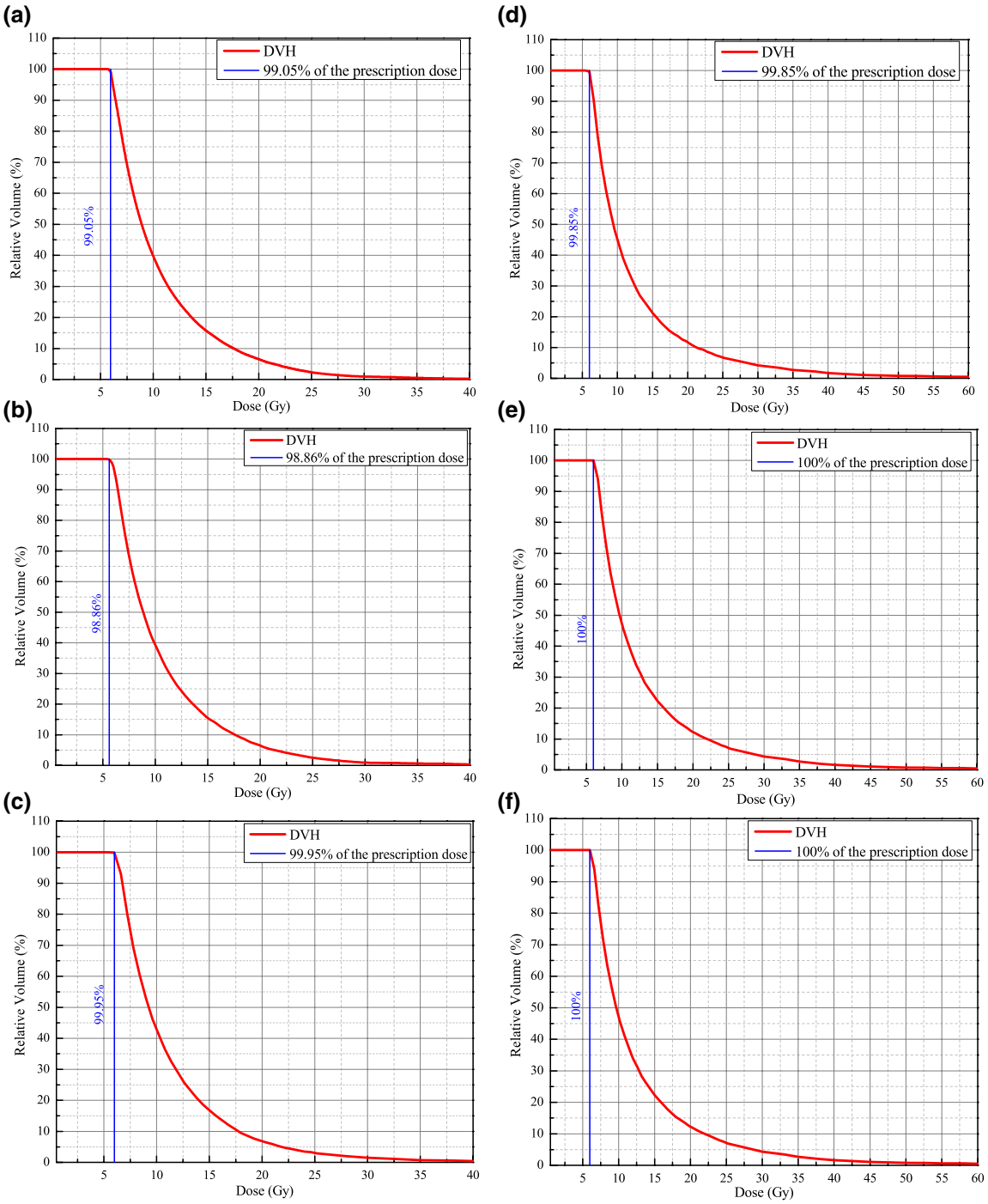

Fig. 8 Cumulative dose-volume histograms (DVHs) for the treatment length of 6 cm. **a**–**c** For target distance of 10 mm. **d**–**f** For the target distance of 15 mm with 2.5, 5 and 10 mm step, respectively

Table 3 Comparison of obtained dose by Monte Carlo calculation (MC) and treatment planning system (TPS) at the anatomical points for the treatment length of 6 cm with 2.5, 5 and 10 mm steps

Stepping size	Target distance of 10 mm					Target distance of 15 mm			
	Dwell index	Dwell times (s)	Dose MC (Gy)	Dose TPS (Gy)	Relative differences (%)	Dwell times (s)	Dose MC (Gy)	Dose TPS (Gy)	Relative differences (%)
2.5 mm	1	51.38	5.81	5.71	1.75	84.28	5.71	5.63	1.42
	2	22.47	6.11	6.03	1.33	49.42	6.01	5.92	1.52
	3	0.30	6.09	6.05	0.66	27.38	6.14	6.05	1.49
	4	1.00	5.99	5.94	0.84	11.37	6.12	6.05	1.16
	5	7.26	5.97	5.91	1.02	0.30	6.04	6.02	0.33
	6	12.23	5.98	5.91	1.18	2.71	6.00	5.92	1.35
	7	15.11	5.99	5.93	1.01	8.15	5.95	5.90	0.85
	8	10.25	6.02	5.95	1.18	18.80	5.96	5.88	1.36
	9	8.38	6.01	5.95	1.01	19.18	5.97	5.90	1.19
	10	5.43	6.00	5.94	1.01	18.93	6.00	5.92	1.35
	11	11.52	5.99	5.94	0.84	18.21	6.02	5.95	1.18
	12	10.83	5.99	5.94	0.84	12.93	6.02	5.96	1.01
	13	10.49	6.00	5.95	0.84	16.05	6.02	5.97	0.84
	14	9.97	6.01	5.94	1.18	20.10	6.00	5.97	0.50
	15	7.61	5.99	5.93	1.01	34.90	5.98	5.95	0.50
	16	9.17	5.98	5.93	0.84	23.87	6.00	5.94	1.01
	17	9.60	6.01	5.94	1.18	23.51	5.97	5.91	1.02
	18	12.79	6.01	5.96	0.84	17.79	6.00	5.89	1.87
	19	10.04	6.01	5.96	0.84	10.86	5.98	5.89	1.53
	20	9.58	5.98	5.93	0.84	0.51	5.99	5.93	1.01
	21	10.41	5.95	5.91	0.68	1.77	6.04	6.03	0.17
	22	1.86	6.00	5.98	0.33	7.96	6.09	6.08	0.16
	23	1.05	6.08	6.04	0.66	30.84	6.08	6.05	0.50
	24	22.56	6.11	6.02	1.50	51.33	6.02	5.92	1.69
	25	49.94	5.82	5.71	1.93	70.66	5.72	5.63	1.60
5 mm	1	71.18	5.96	5.90	1.02	129.20	5.82	5.74	1.39
	2	1.77	6.05	6.04	0.17	38.24	6.16	6.05	1.82
	3	21.81	5.97	5.92	0.84	6.16	6.03	5.97	1.01
	4	19.76	6.01	5.94	1.18	23.14	5.96	5.89	1.19
	5	21.22	6.00	5.94	1.01	38.34	5.98	5.91	1.18
	6	15.75	6.00	5.92	1.35	36.75	6.01	5.94	1.18
	7	21.80	6.00	5.95	0.84	22.44	6.00	5.94	1.01
	8	20.60	5.99	5.94	0.84	31.80	6.01	5.93	1.35
	9	13.15	6.01	5.93	1.35	41.33	5.99	5.91	1.35
	10	28.04	6.00	5.97	0.50	24.43	5.95	5.90	0.85
	11	18.05	5.98	5.89	1.53	0.30	6.03	5.99	0.67
	12	0.30	6.05	5.99	1.00	48.22	6.13	6.08	0.82
	13	72.57	5.96	5.88	1.36	124.07	5.84	5.75	1.57
10 mm	1	72.01	6.00	5.93	1.18	144.84	5.86	5.79	1.21
	2	31.47	6.00	5.89	1.87	49.68	6.10	6.04	0.99
	3	40.32	6.00	5.91	1.52	56.38	5.96	5.91	0.85
	4	37.50	6.00	5.91	1.52	67.95	5.99	5.94	0.84
	5	39.78	6.00	5.91	1.52	55.04	5.96	5.90	1.02
	6	33.23	6.00	5.92	1.35	50.97	6.10	6.04	0.99
	7	70.91	6.00	5.91	1.52	143.99	5.86	5.78	1.38

Table 4 Dose-volume histogram parameters for the treatment length of 6 cm with various source steps and target distances

DVH parameters	Stepping size of 2.5 mm		Stepping size of 5 mm		Stepping size of 10 mm	
	Target distances					
	10 mm (%)	15 mm (%)	10 mm (%)	15 mm (%)	10 mm (%)	15 mm (%)
$V_{100\%}$	99.05	99.85	98.86	100	99.95	100
$D_{100\%}$	98.00	99.70	97.60	100	99.90	100

Compliance with ethical standards

Funding No specific funding was disclosed.

Conflicts of interest The authors declare that they have no conflict of interest.

Research involving human and animal participants This article does not contain any studies with human participants or animals performed by any of the authors.

References

1. Sadeghi M, Enferadi M, Shirazi A (2010) External and internal radiation therapy: past and future directions. J Cancer Res Ther 6(3):239–248
2. Yoshimura R, Hayashi K, Ayukawa F, Toda K, Iwata M, Oota S, Hoshi A, Wakatsuki M, Kurosaki H, Okazaki A, Shibuya H (2008) Radiotherapy doses at special reference points correlate with the outcome of cervical cancer therapy. Brachytherapy 7:260–266
3. Sarabiasl A, Ayoobian N, Poorbaygi H et al (2016) Erratum to: Monte Carlo dosimetry of the IRAsource high dose rate ^{192}Ir brachytherapy source. Australas Phys Eng Sci Med 39:591. https://doi.org/10.1007/s13246-016-0444-z
4. Hirose K, Aoki M, Sato M et al (2016) Jpn J Radiol 34(11):718–723. https://doi.org/10.1007/s11604-016-0578-7
5. Janulionis E, Samerdokiene V, Valuckas KP, Atkocius V, Rivard MJ (2018) Second primary malignancies after high-dose-rate ^{60}Co photon or ^{252}Cf neutron brachytherapy in conjunction with external-beam radiotherapy for endometrial cancer. Brachytherapy 17:768–774
6. Skowronek J (2017) Current status of brachytherapy in cancer treatment—short overview. J Contemp Brachyther 9:581–589
7. Choi CH, Ye SJ, Parsai EI, Shen S, Meredith R, Brezovich IA, Ove R (2009) Dose optimization of breast balloon brachytherapy using a stepping ^{192}Ir HDR source. J Appl Clin Med Phys 10(1):90–102
8. Patel NP, Majumdar B, Hota PK et al (2005) Dose uniformity assessment of intraluminal brachytherapy using HDR ^{192}Ir stepping source. J Can Res Ther 1(2):84–91
9. Morén B, Larsson T, Tedgren ÅC (2018) Mathematical optimization of high dose-rate brachytherapy—derivation of a linear penalty model from a dose-volume model. Phys Med Biol 63(5):065011. https://doi.org/10.1088/1361-6560/aaab83
10. Lahanas M, Baltas D, Zamboglou N (1999) Anatomy-based three-dimensional dose optimization in brachytherapy using multiobjective genetic algorithms. Med Phys 26:1904–1918
11. Giantsoudi D, Baltas D, Karabis A, Mavroidis P, Zamboglou N, Tselis N, Shi C, Papanikolaou N (2013) A gEUD-based inverse planning technique for HDR prostate brachytherapy: feasibility study. Med Phys 40:041704
12. Holm Å, Larsson T, Carlsson Tedgren Å (2013) A linear programming model for optimizing HDR brachytherapy dose distributions with respect to mean dose in the DVH-tail. Med Phys 40:081705
13. De Boeck L, Beliën J, Egyed W (1990) Dose optimization in high-dose-rate brachytherapy: a literature review of quantitative models from 1990 to 2010. Oper Res Health Care. 2014(3):80–90
14. Alber M, Birkner M, Laub W, Nüsslin F (2000) Hyperion—an integrated IMRT planning tool. In: Schlegel W, Bortfeld T (eds) The use of computers in radiation therapy. Springer, Berlin. https://doi.org/10.1007/978-3-642-59758-9_17
15. Chui C-S, Spirou SV (2001) Inverse planning algorithms for external beam radiation therapy. Med Dosim 26(2):189–197
16. Chvetsov A (2005) SU-FF-T-108: computing the regularization parameter for inverse treatment planning using the L-curve method. Med Phys 32:1974–1974. https://doi.org/10.1118/1.1997779
17. Badry H, Oufni L, Ouabi H, Hirayama H (2018) A Monte Carlo investigation of the dose distribution for ^{60}Co high dose rate brachytherapy source in water and in different media. Appl Radiat Isot 136:104–110
18. Sato Sato T et al (2018) Features of particle and heavy ion transport code system (PHITS) version 3.02. J Nucl Sci Technol. https://doi.org/10.1080/00223131.2017.1419890
19. Puchalska M, Sihver L, Sato T, Berger T, Reitz G (2012) Simulations of MATROSHKA experiment at ISS using PHITS. Adv Space Res 50:489–495
20. Sato T, Kase Y, Watanabe R, Niita K, Sihver L (2009) Biological dose estimation for heavy ion therapy using an improved PHITS code coupled with the microdosimetric kinetic model. Radiat Res 171:107–117
21. Ohta M, Nakao N, Kuribayashi S, Hayashizaki N (2018) Verification of evaluation accuracy of absorbed dose in the dose-evaluation system for iridium-192 brachytherapy for treatment of keloids. Biomed Phys. Eng Express 4:025022
22. Badry H, Oufni L, Ouabi H, Hirayama H (2018) Monte Carlo dose calculation for HDR brachytherapy source using EGS5 code. Radiat Phys Chem 150:76–81
23. Rivard MJ, Coursey BM, DeWerd LA, Hanson WF, Huq MS, Ibbott GS, Mitch MG, Nath R, Williamson JF (2004) Update of AAPM task group no. 43 report: a revised AAPM protocol for brachytherapy dose calculations. Med Phys. 31:633–674
24. Bertaccini D, Chan RH, Morigi S, Sgallari F (2012) An adaptive norm algorithm for image restoration. In: Bruckstein AM, ter Haar Romeny BM, Bronstein AM, Bronstein MM (eds) Scale space and variational methods in computer vision. SSVM 2011. Lecture notes in computer science. Springer, Berlin
25. Tikhonov AN (1963) Solution of incorrectly formulated problems and the regularization method. Soviet Math Dokl. 4:1035–1038; English translation of Dokl Akad Nauk. SSSR, 151(1963) pp 501–504

26. Tikhonov AN, Arsenin VY (1977) Solutions of ill-posed problems. Halsted Press, Washington/New York
27. Gfrerer H (1987) An a posteriori parameter choice for ordinary and iterated Tikhonov regularization of ill-posed problems leading to optimal convergences rates. Math Comput 49:507–522
28. Liu Y, Zhang C, Li W et al (2018) An adaptive multiscale anisotropic diffusion regularized image reconstruction method for digital breast tomosynthesis. Australas Phys Eng Sci Med 41:993. https://doi.org/10.1007/s13246-018-0700-5
29. Golub GH, Heath MT, Wahba G (1979) Generalized cross-validation as a method for choosing a good ridge parameter. Technometrics 21:215–223
30. Hansen PC, O'Leary DP (1993) The use of the L-curve in the regularization of discrete ill-posed problems. SIAM J Sci Comput 14:1487–1503
31. Hansen PC (2001) The L-curve and its use in the numerical treatment of inverse problems; invited chapter. In: Johnston P (ed) Computational inverse problems in electrocardiology. WIT Press, Southampton, pp 119–142
32. Gunawan FE, Homma H (2004) Efficient iterative solution for large elasto-dynamic. Inverse problems. JSME Int J 24:130–137

Publisher's Note Springer Nature remains neutral with regard to jurisdictional claims in published maps and institutional affiliations.